

Characterizing monocyte-dependent gene expression in metastatic canine osteosarcoma

Noah Dwyer V'26

Cummings School of Veterinary Medicine at Tufts University

Under the supervision of:

Heather Gardner

DVM, PhD, DACVIM (Oncology)

Department of Clinical Sciences

Signature of Mentor

This summer research was supported, in part, by:

NIH's National Cancer Institute Grant U01CA224182

Student funding was provided by an NIH T35 Grant

Abstract

While metastasis of canine osteosarcoma (OS) predominantly occurs in the lungs, it also develops in subcutaneous tissue, kidneys, and other bones. A role for CCR2 and IL-8 in OS pulmonary metastasis has been identified, but it is unknown whether monocytes play an equally important role in driving the metastatic behavior of OS to alternate metastatic sites¹. NanoString nCounter analysis of gene expression was performed in primary and multiple matched metastatic lesions (lung, kidney, subcutaneous, bone) and identified a predominance of monocyte-associated gene signatures in lung and renal sites when compared to subcutaneous and bone sites. It was therefore hypothesized that monocyte infiltrates are present in renal metastases and that monocyte-associated immunosuppressive gene expression signatures are conserved across patient-matched pulmonary and renal metastatic samples. It was further hypothesized that robust monocyte infiltrates are not present in subcutaneous or bone metastases. The NanoString GeoMX Digital Spatial Profiler was used to analyze and compare the transcriptomes of patient-matched OS metastatic samples collected from dogs and prepared on TMAs. Fluorescent conjugated morphologic antibodies targeting nuclei, vimentin, CD3 T-cells and macrophages were used to guide region of interest selection and to separate monocyte infiltrates from surrounding cell populations. The GeoMx Canine Cancer Panel was hybridized to each slide allowing for analysis of differential expression of genes within selected regions of varying monocyte density at each metastatic site. These findings will help to characterize the role of monocytes in driving OS metastatic behavior in alternate metastatic sites.

Introduction

A recurring clinical challenge associated with osteosarcoma (OS) is the development of multi-drug resistant metastatic disease, which predominantly occurs in the lungs, but also develops in subcutaneous tissue, kidneys, and other bones. Interestingly, a role for the CCL2-CCR2 axis of monocyte recruitment, as well as both IL-6 and IL-8 in OS pulmonary metastasis has been identified^{1,2}. Epigenetic modifications within a subset of primary OS tumor cells lead to aberrant expression of oncogenic gene $\Delta Np63$ ¹. Chemotactic signals from lung tissue promote IL-6 and IL-8 secretion from these mutated OS cells, allowing for colonization of lung tissue, and recruitment of immune cells to the metastatic niche¹. Monocytes expressing CCR2 are preferentially recruited to pulmonary metastatic sites, suggesting an important role for these monocytes in driving the metastatic behavior of OS in the lungs via promotion of neovascularization and immunosuppression¹. Blockade of the CCL2-CCR2 axis with losartan has been associated with clinical benefit in dogs with metastatic OS³⁻⁵. The mounting evidence supporting a role for monocytes in OS metastasis has led to a resurgence in immunotherapy clinical trials designed to evaluate novel approaches targeting the tumor microenvironment. However, it is unknown whether the role of monocytes in driving metastasis is limited to pulmonary metastases, or whether they are similarly important in alternate metastatic sites. NanoString nCounter analysis of gene expression was performed in primary and multiple matched OS metastatic samples (lung, kidney, subcutaneous, bone) and identified a predominance of monocyte-associated gene signatures in lung and renal sites when compared to subcutaneous and bone sites. It is therefore hypothesized that monocyte/macrophage infiltrates are present in renal metastases and that monocyte-associated immunosuppressive gene expression signatures are conserved across patient-matched pulmonary and renal metastatic samples. It is further hypothesized that robust monocyte/macrophage infiltrates are not present in subcutaneous or bone metastases.

Methods

Osteosarcoma tissue samples were collected from primary tumor sites and various metastatic sites (including lung, renal, subcutaneous and bone) of sixty canine patients, of which a subset were selected for analysis. The primary appendicular samples were collected at the time of amputation, while the metastatic samples were collected at the time of patient euthanasia. For Nanostring nCounter analysis, RNA was extracted from flash frozen primary and metastatic tumor samples using the Qiagen RNEasy Mini Plus Extraction Kit per manufacturer guidelines. The Nanostring nCounter Canine IO panel was hybridized to the extracted RNA, and differential gene expressions were quantified using the Nanostring nCounter Max. Results were analyzed using the Nanostring Rosalind platform, with comparisons made between gene expressions of pulmonary metastatic sites and each individual alternate metastatic site (renal, subcutaneous, bone).

For GeoMx Digital Spatial Profiler (DSP) analysis, canine OS tumor samples were paraffin-fixed and formalin embedded (PPFE), then assembled into patient-matched tissue microarrays (TMAs). Four fluorescent conjugated morphologic antibodies targeting Syto 83 (nuclei), vimentin (sarcoma and stromal cells), CD3 (T-Cells) and CD163 (macrophages) were optimized on patient-matched TMAs to guide GeoMx DSP region of interest (ROI) selection. RNAScope was also performed on a subset of patient-matched TMAs following ACD guidelines for RNAScope on bone-derived tissues in order to assess RNA quality prior to subsequent GeoMx DSP analysis.

| Antibody | Clone | Vendor | Fluorophore | Target |
|----------|----------|--------------|---------------|---------------------------|
| Syto 83 | N/A | ThermoFisher | 568/Cy3 | Cell Nucleus |
| Vimentin | RV303 | AbCam | 488/FITC | Sarcoma and Stromal Cells |
| CD3 | C3e/1308 | BioRad | 647/Cy5 | T-Cells |
| CD163 | Edhu-1 | Novus | 594/Texas Red | Monocytes |

Table 1: Antibodies optimized to canine OS TMAs

Results

1. Renal vs. Pulmonary Metastatic OS Samples

Differential gene expression analysis of canine pulmonary and renal OS samples via Nanostring's Rosalind platform revealed a significant ($p=0.05$) differential expression of only four genes among the 800 genes included in the nCounter Canine IO panel. All of these genes were expressed at comparatively lower levels in renal OS tissue when compared to pulmonary. One gene, CD38, has been linked to T-cell inhibition among tumor-promoting monocytes, while other differentially expressed genes were linked to complement activation (C4BPA, MASP1) and T-cell/NK cell antigen presentation (CD2)⁸⁻⁹.

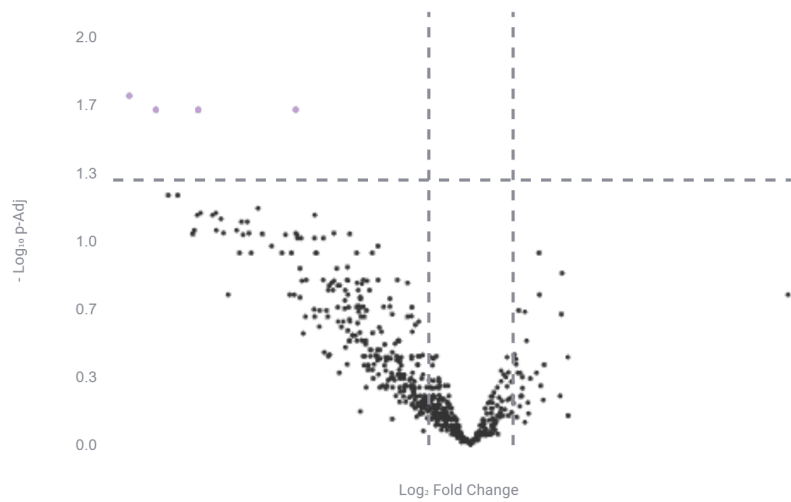


Figure 2: A volcano plot representing the differential expression between canine renal and pulmonary OS metastatic samples among the 800 genes included in the nCounter Canine IO Panel ($p=0.05$).

2. Subcutaneous vs. Renal Metastatic OS Samples

Differential gene expression analysis of canine pulmonary and subcutaneous OS samples via Nanostring's Rosalind platform revealed a significant ($p=0.05$) differential expression of 137 genes among the 800 genes included in the nCounter Canine IO panel, with 135 genes expressed at a comparatively lower level in subcutaneous tissue. Several of these genes are implicated in monocyte/macrophage function. Genes associated with monocyte chemotaxis (CCR2, CCL5, TREM1, and CXCR1) were expressed at a significantly lower level in subcutaneous OS metastases when compared to pulmonary OS metastases, as were genes associated with immunosuppressive macrophage phenotypes (S100A9, IL-19, IL-4R, CCR2, IL6R, SOCS3, JAK2, STAT3)^{1,10-14}. Monocyte immunosuppressive markers (IL-10, MARCO) were also expressed at comparatively lower levels in subcutaneous OS metastatic samples^{15,16}.

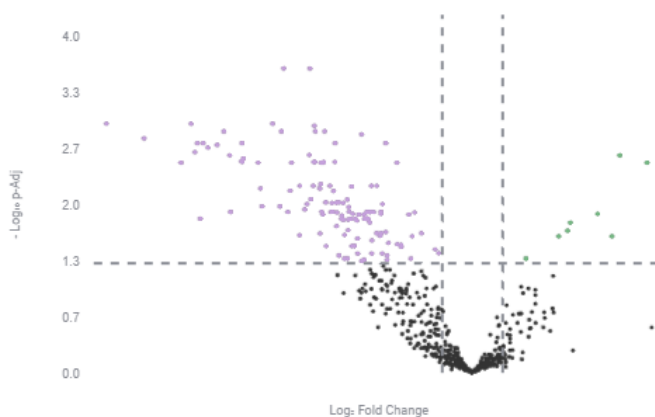


Figure 3: A volcano plot representing the differential expression between canine subcutaneous and pulmonary OS metastatic samples among the 800 genes included in the nCounter Canine IO Panel ($p=0.05$).

3. Bone vs. Renal Metastatic OS Samples

Differential gene expression analysis of canine pulmonary and subcutaneous OS samples via Nanostring's Rosalind platform revealed a significant ($p= 0.05$) differential expression of 131 genes among the 800 genes included in the nCounter Canine IO panel, with 123 genes expressed at a comparatively lower level in OS bone metastatic tissue. Genes associated with monocyte chemotaxis (CCL4, CCL5, and CXCL10) were expressed at a significantly lower level in bone OS metastases when compared to pulmonary OS metastases, as were genes associated with immunosuppressive macrophage phenotypes (ARG2, IL-10, JAK3)^{10,11}. Monocyte markers (IL-10, MARCO, and CD163) were also expressed at comparatively lower levels in bone OS metastatic samples^{15,16}.

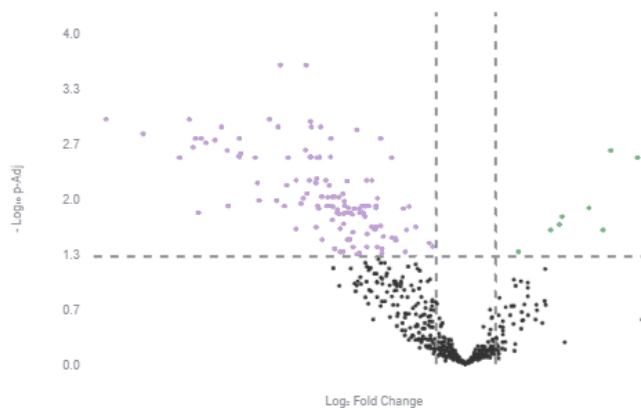


Figure 4: A volcano plot representing the differential expression between canine bone and pulmonary OS metastatic samples among the 800 genes included in the nCounter Canine IO Panel ($p=0.05$).

Discussion

Based on differential gene expression analysis, monocyte-associated gene expression signatures are conserved between OS pulmonary and renal metastatic samples. Monocyte chemotactic markers and immunosuppressive monocyte markers were not differentially expressed at significant levels across the two metastatic sites, perhaps indicating that monocytes maintain their role in driving OS tumor metastases to renal tissues and may also play a role in promoting immunosuppression within the tumor microenvironment⁸⁻¹⁶. These findings are somewhat limited, due to the small sample size of renal metastatic samples available for analysis. Bulk analysis of gene expression does not allow for certainty that the gene expression signatures are definitively derived from monocyte populations, which may be resolved through spatial transcriptomic analysis with the GeoMx DSP.

Monocyte-associated gene expression signatures apparent in OS pulmonary metastatic samples are not observed in subcutaneous and bone metastatic samples, indicating that metastasis to

these sites may not be driven by monocytes⁸⁻¹⁶. More than 100 genes are expressed at significantly lower levels in the subcutaneous and bone samples, with many of these markers relating to immunosuppressive monocyte behavior and polarization⁷. As aforementioned, these findings are limited due to bulk analysis of gene expression and can likely be resolved through use of the GeoMx DSP.

Ultimately, it is hypothesized that monocyte/macrophage infiltrates are present in OS renal metastases and that monocyte-associated immunosuppressive gene expression signatures are conserved across patient-matched pulmonary and renal metastatic samples. It is further hypothesized that robust monocyte/macrophage infiltrates are not present in subcutaneous or bone metastases. Hybridization of the GeoMx Digital Spatial Profiler Canine Cancer Atlas panel to patient-matched TMAs, with morphologic fluorescent antibodies guiding region of interest selection, will allow for the detection of macrophage infiltrates within metastatic canine OS samples, as well as spatial transcriptomic analysis of regions of varying monocyte density across metastatic tissue types. Gene expression of macrophage subsets within each metastatic sample will further illuminate the function of macrophages within the respective tumor microenvironments. This will help to further define the roles that monocytes play in driving and promoting canine OS metastasis at different anatomic sites.

Works Cited

1. Regan et al. The Angiotensin Receptor Blocker Losartan Suppresses Growth of Pulmonary Metastases via AT1R-Independent Inhibition of CCR2 Signaling and Monocyte Recruitment. *J Immunol.* 2019 May 15;202(10):3087-3102. doi: 10.4049/jimmunol.1800619. Epub 2019 Apr 10. PMID: 30971441; PMCID: PMC6504574.
2. Gross et al. IL-6 and CXCL8 mediate osteosarcoma-lung interactions critical to metastasis. *JCI Insight.* 2018 Aug 23;3(16):e99791. <https://doi.org/10.1172/jci.insight.99791>
3. Fei et al. Targeting the CCL2/CCR2 Axis in Cancer Immunotherapy: One Stone, Three Birds? *Front. Immunol* 2021 Nov 03;12:<https://doi.org/10.3389/fimmu.2021.771210>
4. Hao, Q., Vadgama, J.V. & Wang, P. CCL2/CCR2 signaling in cancer pathogenesis. *Cell Commun Signal* 18, 82 (2020). <https://doi.org/10.1186/s12964-020-00589-8>
5. London C et al. 840 Triple-drug oral immunotherapy targeting myeloid cells for treatment of metastatic osteosarcoma evaluated in spontaneous canine model. *Journal for ImmunoTherapy of Cancer.* 2022; 10 Nov 7. doi: 10.1136/jitc-2022-SITC2022.0840
6. Sottnik J.L. et al. Association of Blood Monocyte and Lymphocyte Count and Disease-Free Interval in Dogs with Osteosarcoma. *JVIM.* 2010 Sep;24(6):1439-1444. doi: [10.1111/j.1939-1676.2010.0591.x](https://doi.org/10.1111/j.1939-1676.2010.0591.x)
7. Liu, J., Geng, X., Hou, J. *et al.* New insights into M1/M2 macrophages: key modulators in cancer progression. *Cancer Cell Int* 21, 389 (2021). <https://doi.org/10.1186/s12935-021-02089-2>
8. Karakasheva et al. CD38-Expressing Myeloid-Derived Suppressor Cells Promote Tumor Growth in a Murine Model of Esophageal Cancer. *Cancer Res.* 2015 Oct 1;75(19):4074-85. doi: 10.1158/0008-5472.CAN-14-3639. PMID: 26294209; PMCID: PMC4592477
9. Richards DM, Hettinger J, Feuerer M. Monocytes and macrophages in cancer: development and functions. *Cancer Microenviron.* 2013 Aug;6(2):179-91. doi: 10.1007/s12307-012-0123-x. PMID: 23179263; PMCID: PMC3717063.

10. Chao-Chi H et al. TREM-1 Expression in Tumor-associated macrophages and clinical outcome in lung cancer. *Am. J. Respir. Crit. Care Med.* 2008 Apr;177(7): 763-770. doi: 0.1164/rccm.200704-641OC
11. Yang LF, Zhang ZB, Wang L. S100A9 promotes tumor-associated macrophage for M2 macrophage polarization to drive human liver cancer progression: An in vitro study. *Kaohsiung J Med Sci.* 2023 Apr;39(4):345-353. doi: 10.1002/kjm2.12651. Epub 2023 Feb 21. PMID: 36807724.
12. Zhou D, Chen L, Yang K, Jiang H, Xu W, Luan J. SOCS molecules: the growing players in macrophage polarization and function. *Oncotarget.* 2017 Aug 4;8(36):60710-60722. doi: 10.18632/oncotarget.19940. PMID: 28948005; PMCID: PMC5601173.
13. Xie, Y., Chen, Z., Zhong, Q. et al. M2 macrophages secrete CXCL13 to promote renal cell carcinoma migration, invasion, and EMT. *Cancer Cell Int* 21, 677 (2021). <https://doi.org/10.1186/s12935-021-02381-1>
14. Georgoudaki et al. Reprogramming tumor associated macrophages by antibody targeting inhibits cancer progression and metastasis. *Cell Reports.* 2016 May 31;15:2000-2011. <https://doi.org/10.1016/j.celrep.2016.04.084>
15. Meireson A, Devos M, Brochez L. IDO Expression in Cancer: Different Compartment, Different Functionality? *Front. Immunol.* 2020 Sep 24;11. <https://doi.org/10.3389/fimmu.2020.531491>
16. Dowling, J.K., Afzal, R., Gearing, L.J. et al. Mitochondrial arginase-2 is essential for IL-10 metabolic reprogramming of inflammatory macrophages. *Nat Commun* 12, 1460 (2021). <https://doi.org/10.1038/s41467-021-21617-2>